

AMNS: Attention-Weighted Selective Mask and Noise Label Suppression for Text-to-Image Person Retrieval

^{1st} Runqing Zhang

Shenzhen Institute for Advanced Study

University of Electronic Science and Technology of China
Shenzhen, China

202322280540@std.uestc.edu.cn

^{2nd} Xue Zhou[†]

Shenzhen Institute for Advanced Study

University of Electronic Science and Technology of China
Shenzhen, China

zhouxue@uestc.edu.cn

Abstract—Text-to-image person retrieval aims to retrieve images of person given textual descriptions, and most methods implicitly assume that the training image-text pairs are correctly aligned, but in practice, under-correlated and false-correlated problems arise for image-text pairs due to poor image quality and mislabeling. Meanwhile, the random masking augmentation strategy may incorrectly discard semantic content resulting in the problem of generating noisy matching between image lexical elements and text descriptions. To solve these two problems, we propose a new noise label suppression method and alleviate the problem generated by random mask through an attention-weighted selective mask strategy. In the proposed noise label suppression method, the effect of noise labels is suppressed by preventing the model from being overconfident by considering the inverse KL scatter loss, which is combined with the weight adjustment focal loss to further improve the model's recognition ability on hard samples. On the other hand, Attention-Weighted Selective Mask processes the raw image through the EMA version of the image encoder, retaining some of the tokens with strong semantic associations with the corresponding text descriptions in order to extract better features. Numerous experiments validate the effectiveness of our approach in terms of dealing with noisy problems. The code will be available soon at <https://github.com/RunQing715/AMNS.git>.

Index Terms—Text-to-image person retrieval, cross-modal retrieval, noise suppression, image mask

I. INTRODUCTION

Text-to-image person retrieval utilizes textual descriptions to aid in the retrieval of person images [1]–[3]. Although many effective retrieval methods have been proposed in the field [4]–[10], almost all of them implicitly assume that all input training pairs are correctly aligned. However, in the real world, noise is prevalent due to factors such as environmental disturbances, imprecise linguistic descriptions, mislabeling, or missing information, etc., making it difficult for the idealized assumptions to hold. In addition, the random masking strategy

[11]–[13] in the process of image enhancement may incorrectly discard semantic content, resulting in noisy matching between image patches and text description, and ultimately lead to the degradation of retrieval performance. Therefore, effective noise suppression methods and image masking strategy are crucial for improving the performance of model retrieval.

In particular, some images are mislabeled, or the image quality is too low, but are still treated as positive examples for cross-modal learning, resulting in the model learning the wrong correspondences, a phenomenon known as Noisy Correspondence (NC). To solve this problem, there are two main approaches: sample selection [14]–[17] and robust loss functions [18]–[20]. The former usually utilizes the memory effect of the deep neural networks [21] to progressively differentiate and filter noisy data, but this may require additional computational resources and carry the risk of mistakenly deleting valid data. Comparatively, the latter approach aims to develop noise-tolerance loss functions to improve the robustness of model training against NC.

Therefore, this paper proposes a new cross-modal matching loss named image-text Bidirectional Similarity Distribution Matching (BSDM) loss, which introduces the inverse KL scattering while retaining the forward KL scattering, so that the model does not blindly pursue a perfect match with all the pairs of positive samples when fitting the data, but rather maintains a certain degree of flexibility, thus effectively suppressing the negative impact of noise labeling. And it is complemented by the introduction of a Weight Adjustment Focal Loss (WAF) based to enhance the model's ability to handle hard samples. In addition, to address the problem that random mask may destroy the semantic association between image patches and text description, this paper introduces an Attention-Weighted Selective Mask (AWM) strategy, which aims to optimize the feature extraction process and improve the retrieval performance by accurately retaining the image regions that are strongly correlated with the textual descriptions and reducing the noisy matching. The main contributions and innovations of this paper are as follows:

- We investigate two problems in text-to-image person re-

[†]: Corresponding author

© 2025 IEEE. Personal use of this material is permitted. Permission from IEEE must be obtained for all other uses, in any current or future media, including reprinting/republishing this material for advertising or promotional purposes, creating new collective works, for resale or redistribution to servers or lists, or reuse of any copyrighted component of this work in other works.

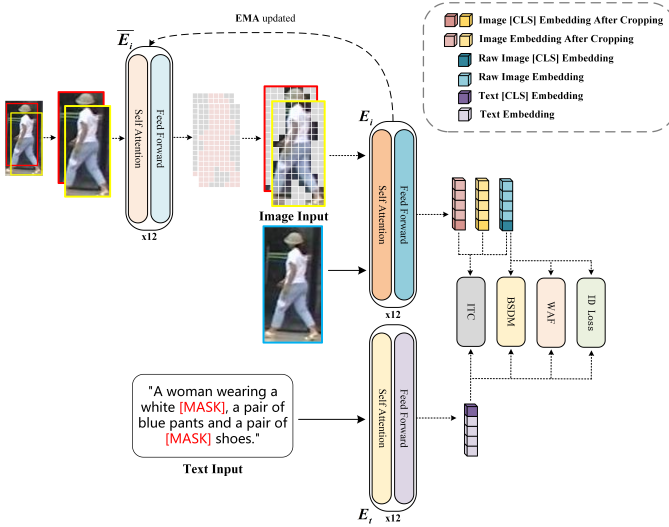


Fig. 1: An overview of our AMNS.

trieval tasks, namely the Noisy Correspondence (NC) and the noisy matching problem caused by random mask strategy. To our knowledge, this paper may be the first to explore the noisy matching problem caused by random mask strategies in pedestrian retrieval tasks.

- We present AMNS: attention-weighted selective mask and noise label suppression framework and introduce an Attention-Weighted Selective Mask (AWM) strategy to alleviate the noisy matching problem caused by random masks. It is proposed that Bidirectional Similarity Distribution Matching (BSDM) can effectively suppress the influence of noise labels, and combined with Weight Adjustment Focal Loss (WAF), The recognition ability of the model on difficult samples is improved.
- Experiments show that AWM strategy is superior to random masking strategy. In addition, the noise suppression method proposed in this paper is applied to other models, and the performance is significantly improved. Among the AMNS methods, mAP index and mINP index are almost the best.

II. METHOD

The overall diagram of our proposed framework is shown in Fig. 1, which consists of an image encoder E_i , a text encoder E_t and an EMA-based image encoder \bar{E}_i . Given an image, crop it and input it to \bar{E}_i , a mask image is obtained using an AWM strategy to highlight image regions relevant to the textual description and fed into E_i together with the raw image, enabling E_i to extract a more accurate representation of the features. The model makes \bar{E}_i filter out features with lower weights by self-supervised learning, and combines with the proposed BSDM, which considers the inverse KL scatter, to inhibit the noisy labelling problem by inversely constraining the true label distribution through the predictive distribution. Meanwhile, combining with the proposed WAF further enhances the model's attention and learning of hard samples by adjusting the weight coefficients. In addition, we adopt ID loss

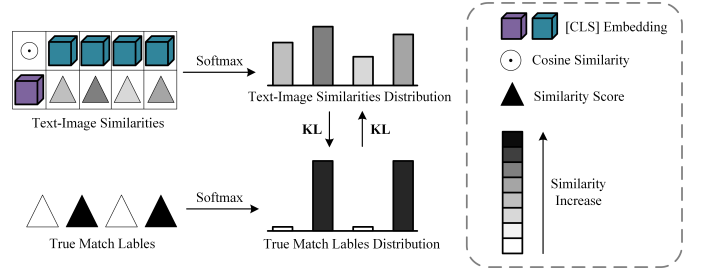


Fig. 2: BSDM diagram. It demonstrates the core idea of implementing noisy label suppression. This approach constrains the true label distribution through the predicted distribution, preventing the model from becoming overconfident and mitigating the impact of noisy labels.

to aggregate feature representations of the same identity, which further improves the model retrieval performance.

A. Attention-Weighted Selective Mask

Since the $[CLS]$ token acts as a representative of global features, it is able to capture the overall semantics of the image and can correspond to the semantics contained in the textual modality. Using this property, we are able to evaluate the relevance of each image region to the overall semantics. Where the attention weight of the token located at position P is:

$$A_P = \frac{1}{HL} \sum_{l=1}^L \sum_{h=1}^H \text{Softmax} \left(\frac{\mathbf{f}_{lh}^q(CLS) \cdot \mathbf{f}_{lh}^k(P)}{\sqrt{d_k}} \right) \quad (1)$$

where l represents the layer index, and h represents the attention head index. $\mathbf{f}_{lh}^q(CLS)$ refers to the query embedding of the $[CLS]$ token at Layer l and Head h . $\mathbf{f}_{lh}^k(P)$ indicates the key embedding of Layer l and Head h for an image token at location P . The variable d_k denotes the dimension of the key. In the overall mask strategy, the sizes of A_P are sorted, and patches with lower weights are filtered out.

For a complete image, we introduce an Exponential Moving Average (EMA) version of the image encoder to generate the attention weights. At the same time, we use the Multiple Views strategy [22], where we take two views and continue to introduce two self-supervised learning methods (SimCLR loss [23] and BYOL loss [24]) to assist in this mask task. Overall, the total loss of the AWM strategy is:

$$L_{AWM} = L_{ITC} + L_{SimCLR} + L_{BYOL} \quad (2)$$

B. Noise Label Suppression Methods

SDM loss [6] effectively differentiates matching from non-matching pairs by aligning the cosine similarity distribution \mathbf{p} of image-text pairs with the ideal label distribution \mathbf{q} . However, due to noisy correspondences in the dataset, SDM forcibly fitting all positive sample pairs of a dataset causes the model to overfit data containing noise.

Therefore, we propose Bidirectional Similarity Distribution Matching (BSDM), the core idea of which is shown in Fig. 2. Building upon the forward KL divergence, BSDM incorporates

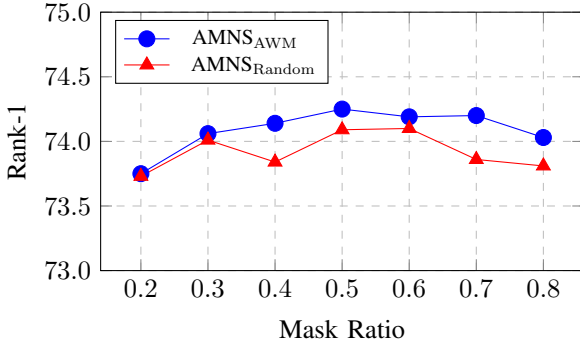


Fig. 3: Variation of Rank-1 performance with different mask ratios for m and τ .

the inverse KL divergence, so that the distribution \mathbf{p} can also exert constraints on the distribution \mathbf{q} . This bidirectional constraint helps alleviate Noisy Correspondences (NC) by allowing the model some flexibility in fitting the data, rather than blindly striving for perfect alignment with all positive pairs.

First, given N image-text pairs, f_i^v and f_j^t denote image global features and text global features. We construct a set of image-text representation pairs as $\{(f_i^v, f_j^t), y_{i,j}\}_{j=1}^N$, where $y_{i,j} = 1$ represents matched pairs from the same identity, and $y_{i,j} = 0$ represents unmatched pairs, $\text{sim}(\mathbf{u}, \mathbf{v}) = \mathbf{u}^T \mathbf{v} / \|\mathbf{u}\| \|\mathbf{v}\|$ denotes the cosine similarity between \mathbf{u} , \mathbf{v} , and τ is the temperature hyperparameter. Then the probability of matching pairs can be calculated using the following softmax function.

$$p_{i,j} = \frac{\exp(\text{sim}(f_i^v, f_j^t)/\tau)}{\sum_{k=1}^N \exp(\text{sim}(f_i^v, f_k^t)/\tau)} \quad (3)$$

The image-to-text \mathcal{L}_{i2t} loss in BSDM is computed by bidirectional KL scattering:

$$\begin{aligned} \mathcal{L}_{i2t} &= KL(\mathbf{p}_i \parallel \mathbf{q}_i) + KL(\mathbf{q}_i \parallel \mathbf{p}_i) \\ &= \frac{1}{N} \sum_{i=1}^N \sum_{j=1}^N \left(p_{i,j} \log \left(\frac{p_{i,j}}{q_{i,j} + \epsilon} \right) + q_{i,j} \log \left(\frac{q_{i,j} + \epsilon}{p_{i,j}} \right) \right) \end{aligned} \quad (4)$$

where ϵ is used to avoid very small numbers in numerical problems. $q_{i,j} = y_{i,j} / \sum_{k=1}^N y_{i,k}$ is the true matching probability. $KL(\mathbf{p}_i \parallel \mathbf{q}_i)$ is the forward KL scatter, and the goal is to make \mathbf{p}_i as close to \mathbf{q}_i as possible, this helps the model to learn the correct data representation. $KL(\mathbf{q}_i \parallel \mathbf{p}_i)$ is the inverse KL scatter. With the bidirectional KL scattering, the model is made to be pushed not only to adapt to the real labels that may contain noise, but also to allow the real labels to adapt to the model's predictions, thus mitigating the effects of NC.

Correspondingly, the loss from text to image \mathcal{L}_{t2i} can be exchanged for f^v and f^t in Eq. (3) (4), BSDM loss is calculated by:

$$\mathcal{L}_{BSDM} = \mathcal{L}_{i2t} + \mathcal{L}_{t2i} \quad (5)$$

TABLE I: Comparison of the performance of the three losses SDM, TAL, and BSDM in the IRRA [6], RDE [37], and AMNS methods on the CUHK-PEDES dataset, where "Best" denotes the selection of the best checkpoints to be tested on the validation set, and the best results are shown in bold. The RDE method continues its performance comparison using two synthetic noise rates, i.e., 20% and 50% to simulate the performance under the real field where the image-text pairs are not well aligned.

Noise	Methods	Loss			CUHK-PEDES					
		SDM	TAL	BSDM	Rank-1	Rank-5	Rank-10	mAP	mINP	
0%	IRRA _{SDM} Best	✓			73.38	89.93	93.71	66.13	50.24	
	IRRA _{TAL} Best		✓		73.20	89.02	93.34	66.05	50.49	
	IRRA _{BSDM} Best			✓	73.51	89.38	93.75	66.27	50.71	
0%	RDE _{SDM} Best	✓			75.26	89.91	94.02	67.37	51.40	
	RDE _{TAL} Best		✓		75.94	90.14	94.12	67.56	51.44	
	RDE _{BSDM} Best			✓	76.06	90.38	94.36	68.04	51.99	
20%	RDE _{SDM} Best	✓			74.27	89.49	93.62	66.34	50.10	
	RDE _{TAL} Best		✓		74.46	89.42	93.63	66.13	49.66	
	RDE _{BSDM} Best			✓	74.95	90.03	94.02	66.88	50.84	
50%	RDE _{SDM} Best	✓			69.33	86.99	91.68	61.99	45.34	
	RDE _{TAL} Best		✓		71.33	87.41	91.81	63.50	47.36	
	RDE _{BSDM} Best			✓	71.33	87.30	92.20	63.75	47.51	
0%	AMNS _{SDM} Best	✓			73.73	89.18	93.55	67.35	52.88	
	AMNS _{TAL} Best		✓		73.39	88.97	93.13	67.17	52.82	
	AMNS _{BSDM} Best			✓	74.25	89.54	93.83	67.67	53.16	

BSDM mitigates the effect of NC by introducing inverse KL scatter, but may weaken the model's learning for hard samples (image-text similarity scores that are low, but are actually positive example samples, or similarity scores that are high, but are actually negative example samples). Therefore, we consider the introduction of focal loss [25] and introduce proportional weight coefficients α, β in front of it to improve it, and by adjusting the coefficient factor γ we are able to adjust the model's attention to the misclassified samples. We refer to this loss as Weight Adjustment Focal Loss (WAF). The image-to-text WAF loss is as follows:

$$\mathcal{L}_{WAF-i2t} = \begin{cases} -\alpha(1 - p_{i,j})^\gamma \log p_{i,j}, & y_{i,j} = 1 \\ -\beta p_{i,j}^\gamma \log(1 - p_{i,j}), & y_{i,j} = 0 \end{cases} \quad (6)$$

Correspondingly, the total WAF loss is as follows:

$$\mathcal{L}_{WAF} = \mathcal{L}_{WAF-i2t} + \mathcal{L}_{WAF-t2i} \quad (7)$$

By combining the two approaches of BSDM and WAF, the model not only suppresses the effect of noisy labels, but also enhances the learning of hard samples, thus achieving better performance in noisy data environments.

Optimization. We also employ the commonly used ID loss [36], whose main purpose is to make feature representations of the same identity clustered together in the feature space, while feature representations of different identities are separated. This helps the model to better distinguish between different entities, thus improving the performance of model retrieval. The overall optimization objective of our training is defined as:

$$\mathcal{L} = \mathcal{L}_{AWM} + \mathcal{L}_{BSDM} + \mathcal{L}_{WAF} + \mathcal{L}_{id} \quad (8)$$

III. EXPERIMENTAL SECTION

A. Datasets and Settings

Datasets: In our experiments, we evaluated the proposed methods on CUHK-PEDES [1], ICFG-PEDES [26], and RST-PReid [27] datasets.

TABLE II: Performance comparison on three datasets. The best and second-best results are in bold and underline, respectively.

Methods	Ref.	CUHK-PEDES					ICFG-PEDES					RSTPReid				
		Rank-1	Rank-5	Rank-10	mAP	mINP	Rank-1	Rank-5	Rank-10	mAP	mINP	Rank-1	Rank-5	Rank-10	mAP	mINP
IVT [30]	ECCVW'22	65.59	83.11	89.21	-	-	56.04	73.60	80.22	-	-	46.70	70.00	78.80	-	-
CFine [32]	TIP'23	69.57	85.93	91.15	-	-	60.83	76.55	82.42	-	-	50.55	72.50	81.60	-	-
PBSL [33]	ACMMM'23	65.32	83.81	89.26	-	-	57.84	75.46	82.15	-	-	47.80	71.40	79.90	-	-
BEAT [34]	ACMMM'23	65.61	83.45	89.54	-	-	58.25	75.92	81.96	-	-	48.10	73.10	81.30	-	-
LCR ² S [19]	ACMMM'23	67.36	84.19	89.62	59.24	-	57.93	76.08	82.40	38.21	-	54.95	76.65	84.70	40.92	-
IRRA [6]	CVPR'23	73.38	<u>89.93</u>	93.71	66.13	50.24	63.46	<u>80.25</u>	85.82	38.06	<u>7.93</u>	60.20	<u>81.30</u>	88.20	47.17	25.28
RDE [37]	CVPR'24	75.94	90.14	94.12	<u>67.56</u>	<u>51.44</u>	67.68	82.47	87.36	<u>40.06</u>	7.87	65.35	83.95	89.90	50.88	28.08
CSKT [8]	ICASSP'24	69.70	86.92	91.80	62.74	-	58.90	77.31	83.56	33.87	-	57.75	<u>81.30</u>	<u>88.35</u>	46.43	-
Our AMNS	-	<u>74.25</u>	89.54	<u>93.83</u>	67.67	53.16	<u>64.05</u>	79.90	<u>85.90</u>	41.27	10.36	<u>60.50</u>	<u>81.30</u>	87.65	<u>47.20</u>	<u>25.38</u>

Evaluation Protocols: For all experiments, we use the popular Rank-K metric (K=1,5,10) to measure retrieval performance. We also use mean Average Precision (mAP) and mean Inverse Negative Penalty (mINP [28]) as auxiliary retrieval metrics to further evaluate the performance.

Implementation Details: In our experiments, we used the same version of CLIP-ViT-B/16 as IRRA [6]. Image augmentation includes color jitter, random horizontal flipping, random crop with padding, random grayscale, random erasing, and gaussian blur. Text augmentation involves random masking, replacement, and removal of word tokens. The model training parameters follow IRRA, the temperature parameter τ of BSDM is set to 0.02, γ of WAF is set to 2, and the values of α and β are set to 0.1 and 0.05, respectively. \bar{E}_i generates an attention mask with a momentum that starts from 0.996 and gradually increases to 1 with training, and the experiments show that it works best when the mask rate is 0.5. Specific experimental results are detailed in Section III-B.

B. Experimental results

In Fig. 3, the experimental results on AMNS show that the effect of attention-weighted selective mask based on attention is generally better than that of random mask, and the effect of attention-weighted selective mask reaches the optimal effect when the mask ratio = 0.5. Therefore, in the subsequent experiments, for the AWM strategy, we all set the mask ratio to 0.5 for the experiments.

As shown in Table I, the SDM loss is the similarity distribution matching loss proposed by IRRA [6], which is introduced in Section II-B. TAL loss is a novel triplet alignment loss proposed by RDE [37], which effectively solves the problem of poor local minima and even model collapse under NC in the early stage of training and achieves better performance. The BSDM is the bidirectional similarity distribution matching loss proposed in this paper. Table I shows that the use of BSDM loss in different methods can bring significant improvement in all aspects of performance, and the best performance is still achieved under the 20% and 50% noise rates, which fully indicates that the BSDM loss proposed by us is superior to the widely used TAL loss and SDM loss, and has better stability and robustness for NC.

Table II shows that our method achieves good results in Rank metrics, and the mAP index and mINP index achieve the best results in the first and second datasets. Higher mINP metrics mean that the correctly matched images are indexed

TABLE III: Ablation study on each component of AMNS on CUHK-PEDES.

No.	Methods	Components			CUHK-PEDES				
		BSDM	WAF	L_{id}	Rank-1	Rank-5	Rank-10	mAP	mINP
0	Baseline				69.12	87.02	92.02	62.17	46.08
1	+BSDM	✓			73.34	89.23	93.02	65.25	48.76
2	+WAF		✓		71.74	88.09	92.56	64.94	49.35
3	+ L_{id}			✓	66.57	85.62	91.00	61.12	45.82
4	+WAF+ L_{id}		✓	✓	69.83	86.11	91.55	65.28	52.07
5	+BSDM+WAF	✓	✓		73.60	88.81	93.11	65.56	49.21
6	+BSDM+ L_{id}	✓		✓	74.16	89.02	93.52	67.37	52.57
7	AMNS	✓	✓	✓	74.25	89.54	93.83	67.67	53.16

at a more advanced position, which fully validates that our method is better at finding all the correct matches and can be better used in real-life retrieval systems.

C. Ablation experiments

In this section, we fine-tune the CLIP-ViT-B/16 model with AWM loss as a baseline and perform ablation studies on the CUHK-PEDES dataset.

Effectiveness of BSDM: As can be seen from No.1 in Table III, just by adding BSDM to Baseline, the accuracies of Rank-1, Rank-5, and Rank-10 are improved by 4.22%, 2.21%, and 1.00%, respectively, and the values of mAP and mINP are improved by 3.08% and 2.68%, respectively, which is a good illustration of the BSDM's Person Retrieval task in terms of its Effectiveness.

Complementarity between BSDM and WAF: As can be seen from No.5 in Table III, the addition of WAF improves the Rank1 metric by 0.26%, and the mAP and mINP metrics by 0.31% and 0.45%, respectively, which fully demonstrates that WAF further improves the model's ability to recognize hard samples when it is complemented with BSDM.

IV. CONCLUSION

In this paper, we explore Noise Correspondence (NC) and the noisy matching problem caused by random masking strategy. We introduce Attention-Weighted Selective Mask to alleviate the noisy matching problem caused by random masking strategy, and propose a novel method, that is, Bidirectional Similarity Distribution Matching method, combined with the improved focal loss, effectively deal with the NC, and achieve excellent performance. We have carried out extensive experiments, which fully prove the superiority of the proposed method in solving the above problems, and prove that our method can find all the correct matches better.

REFERENCES

- [1] Li S, Xiao T, Li H, et al. Person search with natural language description[C]//Proceedings of the IEEE conference on computer vision and pattern recognition. 2017: 1970-1979.
- [2] Wang C, Luo Z, Lin Y, et al. Text-based Person Search via Multi-Granularity Embedding Learning[C]//IJCAI. 2021: 1068-1074.
- [3] Niu K, Liu Y, Long Y, et al. An Overview of Text-based Person Search: Recent Advances and Future Directions[J]. IEEE Transactions on Circuits and Systems for Video Technology, 2024.
- [4] Shu X, Wen W, Wu H, et al. See finer, see more: Implicit modality alignment for text-based person retrieval[C]//European Conference on Computer Vision. Cham: Springer Nature Switzerland, 2022: 624-641.
- [5] Shao Z, Zhang X, Fang M, et al. Learning granularity-unified representations for text-to-image person re-identification[C]//Proceedings of the 30th acm international conference on multimedia. 2022: 5566-5574.
- [6] Jiang D, Ye M. Cross-modal implicit relation reasoning and aligning for text-to-image person retrieval[C]//Proceedings of the IEEE/CVF Conference on Computer Vision and Pattern Recognition. 2023: 2787-2797.
- [7] Cao M, Bai Y, Zeng Z, et al. An empirical study of clip for text-based person search[C]//Proceedings of the AAAI Conference on Artificial Intelligence. 2024, 38(1): 465-473.
- [8] Liu Y, Li Y, Liu Z, et al. CLIP-based Synergistic Knowledge Transfer for Text-based Person Retrieval[C]//ICASSP 2024-2024 IEEE International Conference on Acoustics, Speech and Signal Processing (ICASSP). IEEE, 2024: 7935-7939.
- [9] Wang D, Yan F, Wang Y, et al. Fine-grained Semantics-aware Representation Learning for Text-based Person Retrieval[C]//Proceedings of the 2024 International Conference on Multimedia Retrieval. 2024: 92-100.
- [10] Zuo J, Zhou H, Nie Y, et al. UFineBench: Towards Text-based Person Retrieval with Ultra-fine Granularity[C]//Proceedings of the IEEE/CVF Conference on Computer Vision and Pattern Recognition. 2024: 22010-22019.
- [11] He K, Chen X, Xie S, et al. Masked autoencoders are scalable vision learners[C]//Proceedings of the IEEE/CVF conference on computer vision and pattern recognition. 2022: 16000-16009.
- [12] Zhang C, Zhang C, Song J, et al. A survey on masked autoencoder for self-supervised learning in vision and beyond. arXiv 2022[J]. arXiv preprint arXiv:2208.00173.
- [13] Hondru V, Croitoru F A, Minaee S, et al. Masked Image Modeling: A Survey[J]. arXiv preprint arXiv:2408.06687, 2024.
- [14] Zhang H, Yang Y, Qi F, et al. Robust video-text retrieval via noisy pair calibration[J]. IEEE Transactions on Multimedia, 2023, 25: 8632-8645.
- [15] Han H, Miao K, Zheng Q, et al. Noisy correspondence learning with meta similarity correction[C]//Proceedings of the IEEE/CVF Conference on Computer Vision and Pattern Recognition. 2023: 7517-7526.
- [16] Li J, Li D, Xiong C, et al. Blip: Bootstrapping language-image pre-training for unified vision-language understanding and generation[C]//International conference on machine learning. PMLR, 2022: 12888-12900.
- [17] Zuo J, Yu C, Sang N, et al. Plip: Language-image pre-training for person representation learning[J]. arXiv preprint arXiv:2305.08386, 2023.
- [18] Qin Y, Sun Y, Peng D, et al. Cross-modal active complementary learning with self-refining correspondence[J]. Advances in Neural Information Processing Systems, 2023, 36: 24829-24840.
- [19] Yan S, Dong N, Liu J, et al. Learning comprehensive representations with richer self for text-to-image person re-identification[C]//Proceedings of the 31st ACM international conference on multimedia. 2023: 6202-6211.
- [20] Hu P, Huang Z, Peng D, et al. Cross-modal retrieval with partially mismatched pairs[J]. IEEE Transactions on Pattern Analysis and Machine Intelligence, 2023, 45(8): 9595-9610.
- [21] Arpit D, Jastrzebski S, Ballas N, et al. A closer look at memorization in deep networks[C]//International conference on machine learning. PMLR, 2017: 233-242.
- [22] Yang Y, Huang W, Wei Y, et al. Attentive mask clip[C]//Proceedings of the IEEE/CVF International Conference on Computer Vision. 2023: 2771-2781.
- [23] Chen T, Kornblith S, Norouzi M, et al. A simple framework for contrastive learning of visual representations[C]//International conference on machine learning. PMLR, 2020: 1597-1607.
- [24] Grill J B, Strub F, Altché F, et al. Bootstrap your own latent-a new approach to self-supervised learning[J]. Advances in neural information processing systems, 2020, 33: 21271-21284.
- [25] Lin T Y, Goyal P, Girshick R, et al. Focal loss for dense object detection[C]//Proceedings of the IEEE international conference on computer vision. 2017: 2980-2988.
- [26] Ding Z, Ding C, Shao Z, et al. Semantically self-aligned network for text-to-image part-aware person re-identification[J]. arXiv preprint arXiv:2107.12666, 2021.
- [27] Zhu A, Wang Z, Li Y, et al. Dssl: Deep surroundings-person separation learning for text-based person retrieval[C]//Proceedings of the 29th ACM international conference on multimedia. 2021: 209-217.
- [28] Ye M, Shen J, Lin G, et al. Deep learning for person re-identification: A survey and outlook[J]. IEEE transactions on pattern analysis and machine intelligence, 2021, 44(6): 2872-2893.
- [29] Farooq A, Awais M, Kittler J, et al. Axm-net: Implicit cross-modal feature alignment for person re-identification[C]//Proceedings of the AAAI conference on artificial intelligence. 2022, 36(4): 4477-4485.
- [30] Shu X, Wen W, Wu H, et al. See finer, see more: Implicit modality alignment for text-based person retrieval[C]//European Conference on Computer Vision. Cham: Springer Nature Switzerland, 2022: 624-641.
- [31] Shao Z, Zhang X, Ding C, et al. Unified pre-training with pseudo texts for text-to-image person re-identification[C]//Proceedings of the IEEE/CVF International Conference on Computer Vision. 2023: 11174-11184.
- [32] Yan S, Dong N, Zhang L, et al. Clip-driven fine-grained text-image person re-identification[J]. IEEE Transactions on Image Processing, 2023.
- [33] Shen F, Shu X, Du X, et al. Pedestrian-specific bipartite-aware similarity learning for text-based person retrieval[C]//Proceedings of the 31st ACM International Conference on Multimedia. 2023: 8922-8931.
- [34] Ma Y, Sun X, Ji J, et al. Beat: Bi-directional one-to-many embedding alignment for text-based person retrieval[C]//Proceedings of the 31st ACM International Conference on Multimedia. 2023: 4157-4168.
- [35] Fujii T, Tarashima S, Bilma: Bidirectional local-matching for text-based person re-identification[C]//Proceedings of the IEEE/CVF International Conference on Computer Vision. 2023: 2786-2790.
- [36] Zheng Z, Zheng L, Garrett M, et al. Dual-path convolutional image-text embeddings with instance loss[J]. ACM Transactions on Multimedia Computing, Communications, and Applications (TOMM), 2020, 16(2): 1-23.
- [37] Qin Y, Chen Y, Peng D, et al. Noisy-correspondence learning for text-to-image person re-identification[C]//Proceedings of the IEEE/CVF Conference on Computer Vision and Pattern Recognition. 2024: 27197-27206.